Single Nuclei RNA Sequencing of Mice Hippocampus to Evaluate *in vivo* Gene Editing by a Biodegradable Nanocage for CRISPR/Cas9 Ribonucleoproteins

by

Alex Shintaro Araki

B.S., University of Wisconsin – Madison, 2021

Abstract:

In recent years, CRISPR-Cas9 technology has shown promise as a versatile gene editing tool that enables precise nucleotide base-editing (Sander & Joung, 2014), and are anticipated to drive the next wave of gene therapies for a range of health conditions, including neurodegenerative diseases. However, a major challenge in gene therapy development is in the generation of safe and efficient non-viral delivery devices for *in vivo* Cas9-mediated gene editing. To date, very few safe and effective non-viral Cas9 *in vivo* delivery methods have been reported, with most *in vivo* Cas9 delivery methods utilizing *viral* vectors that require extended manufacturing times with questionable safety profiles and limited packing capacity (Miller et al., 2017). To address these challenges, we have applied a previously developed nanocage (NC) design for non-viral *in vivo* Cas9 ribonucleoprotein (RNP) delivery in mice brain. *In vivo* editing efficiency of RNPs delivered with this NC (NC-RNPs) was evaluated in the hippocampi of Ai14 tdTomato reporter mice using single nuclei RNA sequencing. Seurat integrated differential gene expression analyses between NC-RNP Ai14 targeting experimental and NC-RNP scramble control hippocampi conditions revealed a 2.8 fold increase in tdTomato expression in Ai14 targeting NC-RNP, indicating targeted editing at the Ai14 locus. Upregulated tdTomato expression was observed in all cell types in the hippocampal injection area, suggesting high penetrance of our NC-RNP formulation. Further cluster annotation and gene expression analyses revealed no new immune cell activity between experimental and control conditions, thereby supporting the safety of the NC for *in vivo* Cas9-RNP delivery. While future RNAscope assays are necessary to confirm gene signatures we found through snRNA-seq analyses, our data indicates a safe and robust non-viral Cas9-RNP delivery method for *in vivo* brain editing.

Introduction

In recent years, CRISPR-Cas9 has shown promise as a revolutionary tool for versatile and robust gene editing that can be used as one-time therapeutic cures for treating certain diseases by inducing permanent genetic changes in a sequence-specific manner (Sander & Joung, 2014). Cas9 mediated somatic gene editing therapy is therefore thought to be the next wave for treating various diseases, including neurodegenerative disease. However, current *in vivo* delivery methods for Cas9 gene editing poses several challenges (Mout et al., 2017). To date, most *in vivo* Cas9-based gene editing relies on viral vectors that require laborious manufacturing protocols. These vectors have

questionable safety profiles including off-target edits from continuous Cas9 expression and rare but dangerous integration events that can lead to oncogenesis (Miller et al., 2017). Other alternative delivery methods including electroporation, lipofection and microinjection, all face unique hurdles that make *in vivo* application difficult (Yin et al., 2017). Furthermore, Cas9 delivery to the brain presents additional challenges due to the blood-brain-barrier and the brain's dense parenchymal structure that makes targeted delivery difficult (Martinez et al., 2011). Therefore, there is an urgent need for a non-viral delivery vector for targeted Cas9 delivery into neurons for neurodegenerative disease application.

The Sarah Gong and Krishanu Saha lab at the University of Wisconsin-Madison previously developed a biodegradable nanocage (NC) that encapsulates and delivers a CRISPR-Cas9 ribonucleoprotein (RNP) for gene editing in retinal pigmental epithelium (Chen et al., 2019) (Fig. 1). The NC is composed of imidazole monomers that facilitate endosomal escape, with covalently crosslinked, yet GSH cleavable linkers (N,N'-bis(acryloyl)cystamine) that allows the release of RNPs in GSH-rich cytosols while maintaining structural integrity extracellularly (Chen et al., 2019). The outer water-soluble poly(ethylene glycol) shell provides a structure that allows additional conjugation of an acrylated PEG-ligand, which allows further modification for NC penetration into neurons.

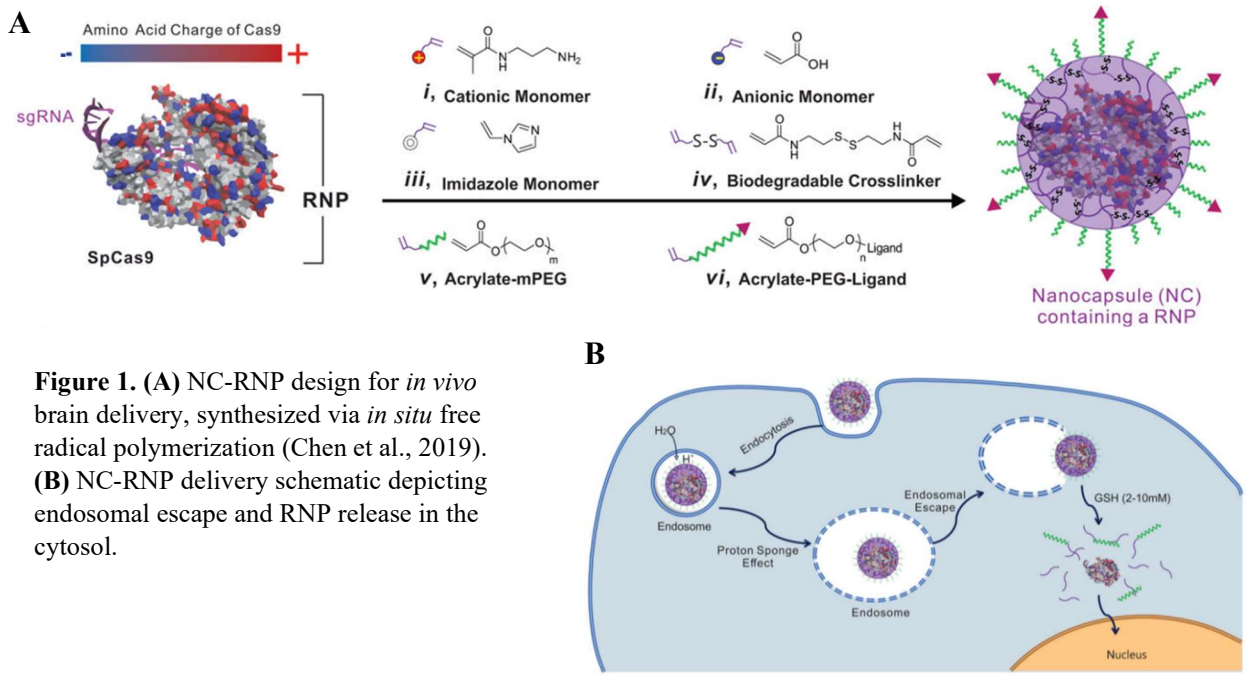

Figure 1. (A) NC-RNP design for *in vivo* brain delivery, synthesized via *in situ* free radical polymerization (Chen et al., 2019). **(B)** NC-RNP delivery schematic depicting endosomal escape and RNP release in the cytosol.

In this paper, we report the successful application of a previously developed NC-RNP formulation for robust and targeted hippocampus editing in mice. The NC-RNP was administered via stereotactic injection into the hippocampus region of an Ai14 tdTomato mouse model with a loxP-STOP cassette that inhibits red fluorescence expression (Fig. 2). Successful NC-RNP editing of two or more poly(A) repeat sequences at the Ai14 locus allows tdTomato expression for robust, high-throughput quantitative analysis with a gain-of-function fluorescent signal in edited cells.

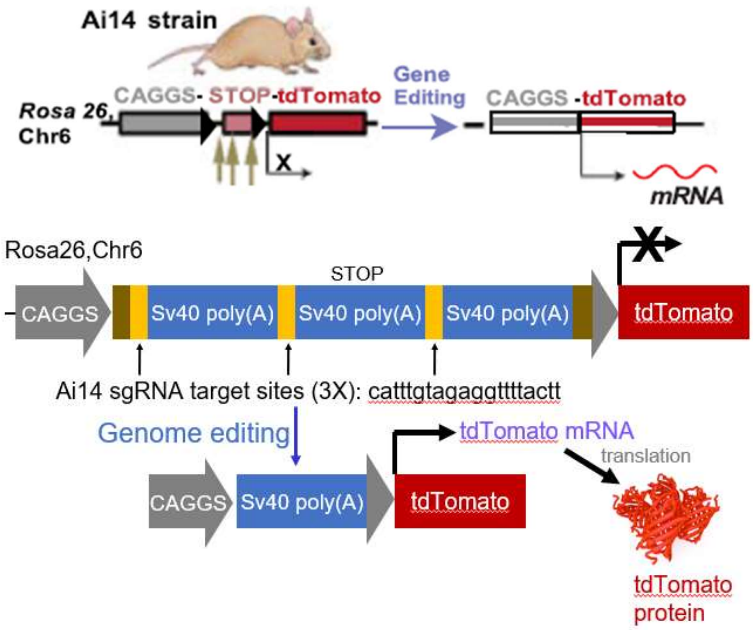

Figure 2. Schematic of Ai14 mouse with tdTomato transgene insert. A STOP cassette consisting of three *Sv40-polyA* sequences halt gene expression downstream of red fluorescence protein.

To examine the effects of the NC-RNP at the single cell resolution, gene expression analysis was performed via single nuclei RNA-seq (snRNA-seq) of Ai14 mice hippocampi. After Illumina 10X sequencing, the data was aligned via CellRanger using an Ai14 tdTomato custom reference genome and analyzed via Seurat R package. Two mouse hippocampi pairs were analyzed using Seurat integrated analysis (Stuart et al., 2019) to reveal an upregulation of our reporter in almost all cell types with no observable immunogenic markers, indicating a safe and robust method for *in vivo* Cas9 mediated gene editing in mouse hippocampi.

Results:

Integrated Seurat analysis reveals 12 distinct cell types and increased tdTomato expression by NC-RNP editing

Integrated analysis of Mouse 1 with NC-RNP scramble control and NC-RNP Ai14 targeting experimental hippocampi conditions revealed 12 distinct cell types (Fig. 3) with 2.8 fold increase in tdTomato positive cells by NC-RNP editing in almost all cell types. Further analysis revealed successful NC-RNP editing in almost all cell types with high selectivity towards pyramidal neurons, with 89.9% of cells within the pyramidal cluster expressing tdTomato

compared to 64.6% in all “Treated” experimental cell types (Fig. 4). After removing positive control fibroblast clusters from the “Treated” condition in Mouse 1, we found 55.2% of all treated cells expressing our reporter compared to 19.5% in the control. The significant increase in expression indicates the robustness of our NC-RNP formulation for hippocampus cell editing.

Integrated analysis of Mouse 2 without positive control fibroblasts revealed an 1.69 fold increase in overall tdTomato expression, with 31.2% of all treated cells and 18.5% of controls expressing our reporter. Featureplot visualizations showed selectivity for cluster 2, with 50.4% of cells within the cluster expressing tdTomato compared to an average of 21% across all other cell types. While cluster 2 has been identified as a hippocampus cell type, it will require more rigorous manual annotation to identify the specific cell type. The increase in reporter gene expression across all cell types in both conditions suggests that our NC-RNP formulation has high penetrance with the capability to deliver our RNP in a variety of different cell types. While more rigorous cluster identification will be required to elucidate the edited cell types, the level of NC-RNP penetrance is similar between both mice.

Immunohistochemistry and Seurat analysis on Mice 1 and 2 showed no significant immune cell marker expression, suggesting the safety of our NC-RNP formulation. UMAP projections of Mouse 1 split by treatment type also showed no new clusters between treatments, providing additional evidence to suggest our NC-RNP formulation does not recruit new immune cell types following RNP delivery (Fig. 6). More rigorous computational analysis of gene lists between cluster types for mice 1 and 2, in addition to the two remaining mouse conditions, are expected to confirm our findings. In addition, the gene signatures found through snRNA-seq analyses will guide future RNAscope assays that will also confirm our data.

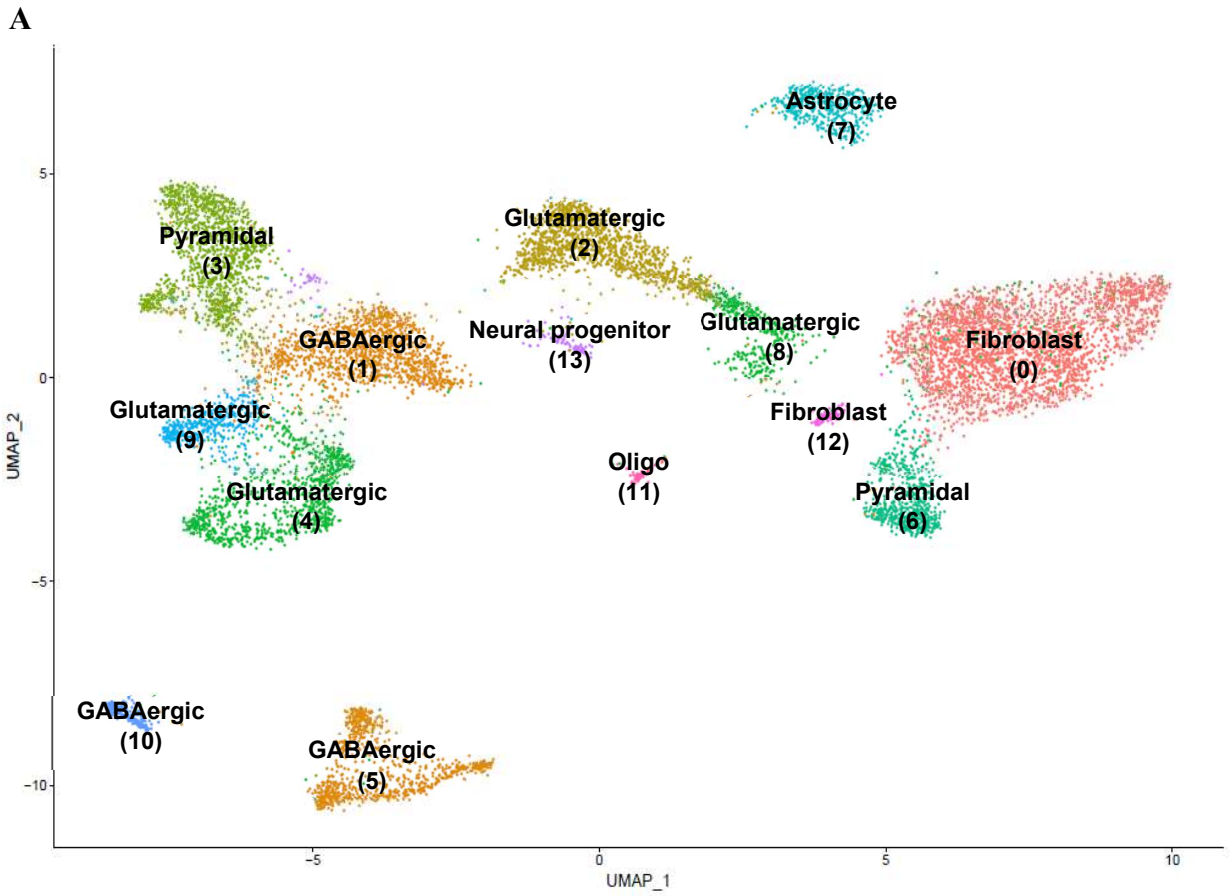

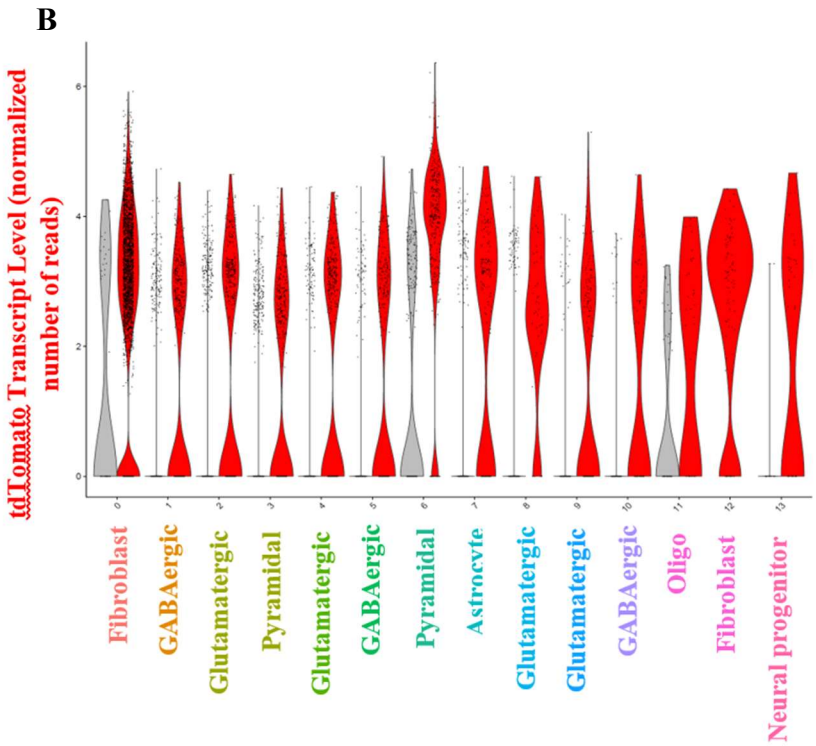

Figure 3. (A) Cell type identification and tdTomato reporter transcript levels of Mouse 1 hippocampi (A) Annotated integrated UMAP projection of Mouse 1 reveals 12 distinct cell types between experimental and control conditions. Clusters 0 and 12 were identified as positive control fibroblast spike.

(B) Transcript Levels for tdTomato-positive nuclei in each cell type of Mouse 1 integrated hippocampi dataset. Grey bars "Control" NC-RNP Scrambled guide condition. Red bar as "Experimental" NC-RNP with Ai14 targeting guide with spike-in of edited fibroblast control nuclei (n =5,307 nuclei).

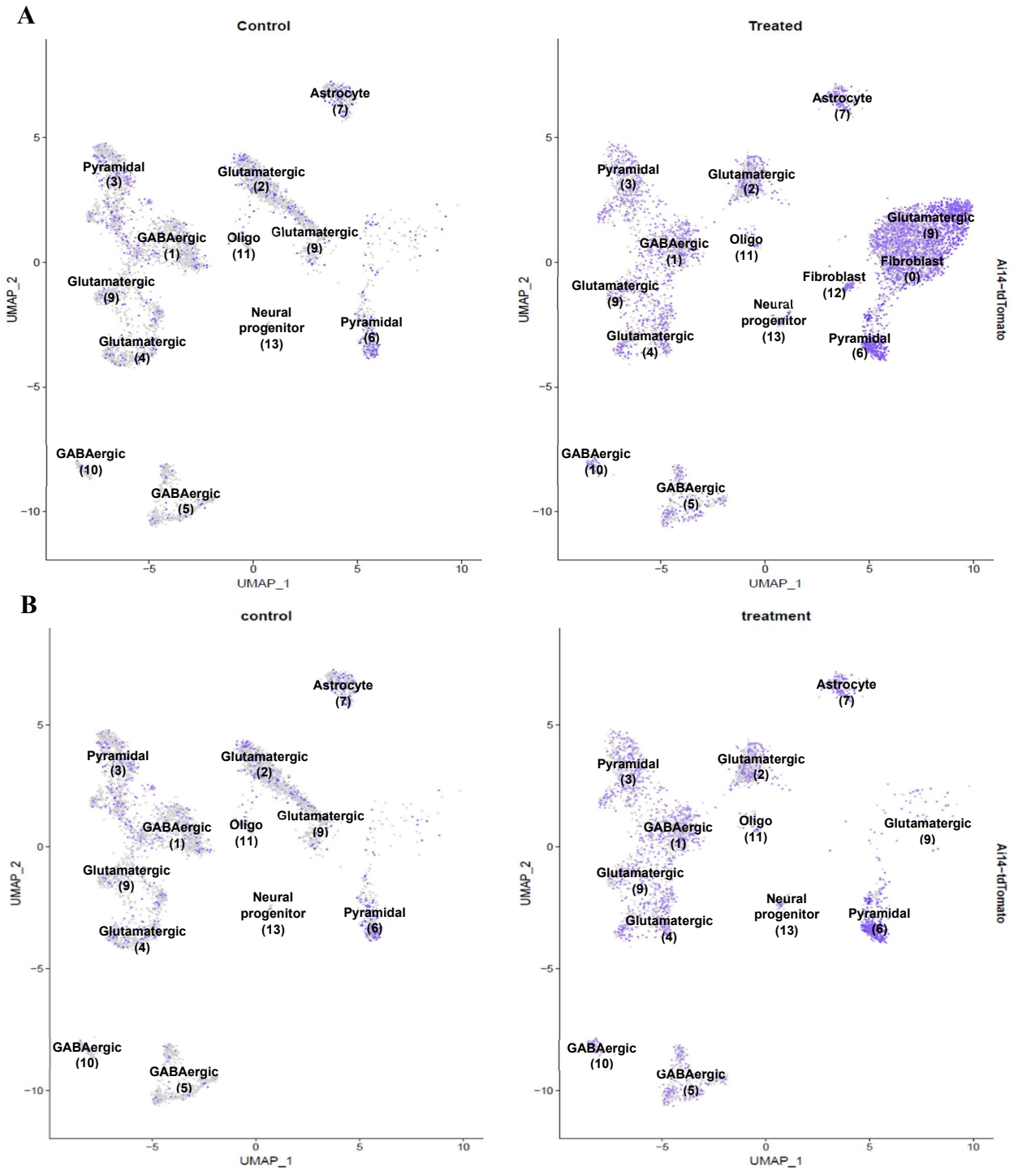

Figure 4. (A) Feature plot of Mouse 1 Fibroblast+ UMAP indicating tdTomato transcript levels and percentage of cells expressing tdTomato in each sample using FindMarkers. **(B)** Feature plot of Mouse 1 Fibroblast-removed UMAP shows tdTomato expressing cell types from NC-RNP editing.

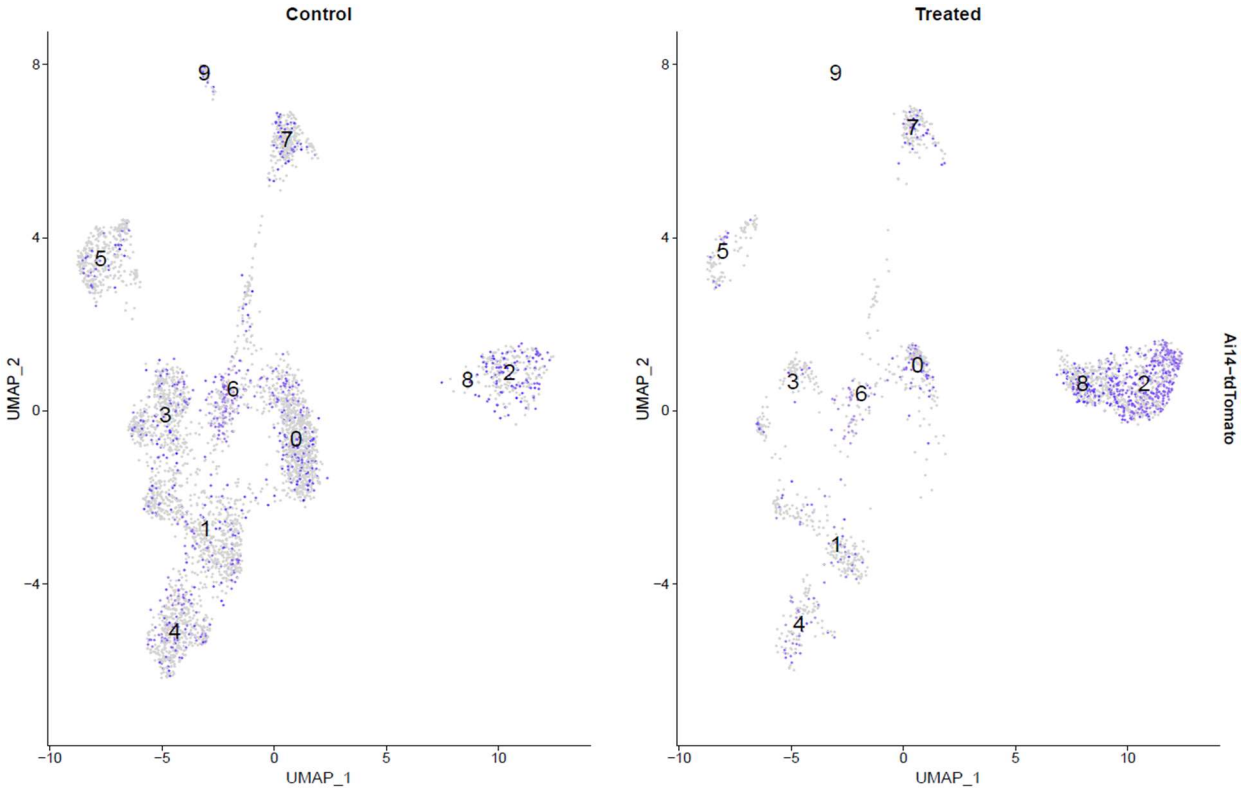

Figure 5. Unenriched UMAP projection of Mouse 2, with tdTomato expression in cluster 2, which has been identified as a hippocampus cell type. More rigorous manual annotation will be required to confidently identify cluster.

Discussion

In this paper, we employed single nuclei RNA-sequencing on Ai14 mice hippocampi to evaluate *in vivo* brain editing by our NC-RNP. Using Seurat integrated analysis, we fully analyzed the hippocampi pair of Mouse 1 and partially analyzed that of Mouse 2. Between Mouse 1 and 2, Seurat analysis reported an average 2.2 fold increase in reporter expression, with 42% of hippocampus cells treated with our NC-RNP expressing tdTomato. Sporadic tdTomato expression was observed in an average of 19.1% of all cells in both control conditions (Fig. 4 & 5). However, our previous microscopy images that showed no signs of tdTomato expression suggest that the calculated expression level is due to ectopic expression of the STOP cassette, and not from the NC-RNP scramble.

Immunohistochemistry and gene enrichment in Seurat revealed no significant immune cell activity with no significant immune cell marker expression. However, we observed Glutamatergic

neurons (8) clusters in Mouse 1 to be shifted in the UMAP space, suggesting a potential cell response to the NC-RNP. In Mouse 2, we also observed significantly more cells in cluster 2 (Fig. 5), which can potentially be another cell response to the NC-RNP. Despite these shifts observed in the UMAP, the lack of a new cluster suggests that there is no significant immunogenic response from the NC-RNP treatment. More precise annotation of clusters using other tools like Allen Brain Atlas (Lein et al., 2006) and rigorous manual identification of cell subtypes will elucidate the *in vivo* effects of our NC-RNP. In future analyses, we will run integrated analyses on two more mouse conditions to evaluate mice-specific differences in cell response to determine immunogenic effects with more confidence.

For spatial mapping and confirmation of gene signatures in our snRNA-seq datasets, we will employ RNAscope, a multiplexed *in situ* hybridization technique that allows for highly specific and sensitive detection of RNAs using a proprietary Z shaped probe (Sheldon et al., 2020). The cell type markers used in snRNA-seq analyses will guide this assay to confirm gene signatures and help identify minor cell populations in our samples. The assay will also allow us to spatially resolve gene expression patterns by visualizing markers in the tissue context (Fig. 7). Lastly, we will explore the impacts of editing at disease relevant endogenous loci such as *APP* to determine the efficacy of our NC-RNP formulation for Alzheimer Disease therapy development.

In this paper, we apply snRNA-seq technology as a method to evaluate the safety, targeting efficiency, and penetrance of a non-viral vector for CRISPR-Cas9 RNP delivery. This approach can be readily applied to evaluate cell-specific effects of various editing strategies and delivery vehicles for novel gene therapies. While gene expression profiling methods have some limitations in spatial mapping for visualizing editing, additional assays such as RNAscope can elucidate gaps in the data to reveal cell-specific effects of gene-editing in tissue contexts. In future studies, we anticipate snRNA-seq to aid the development of *in vivo* gene therapies for neurodegenerative disease.

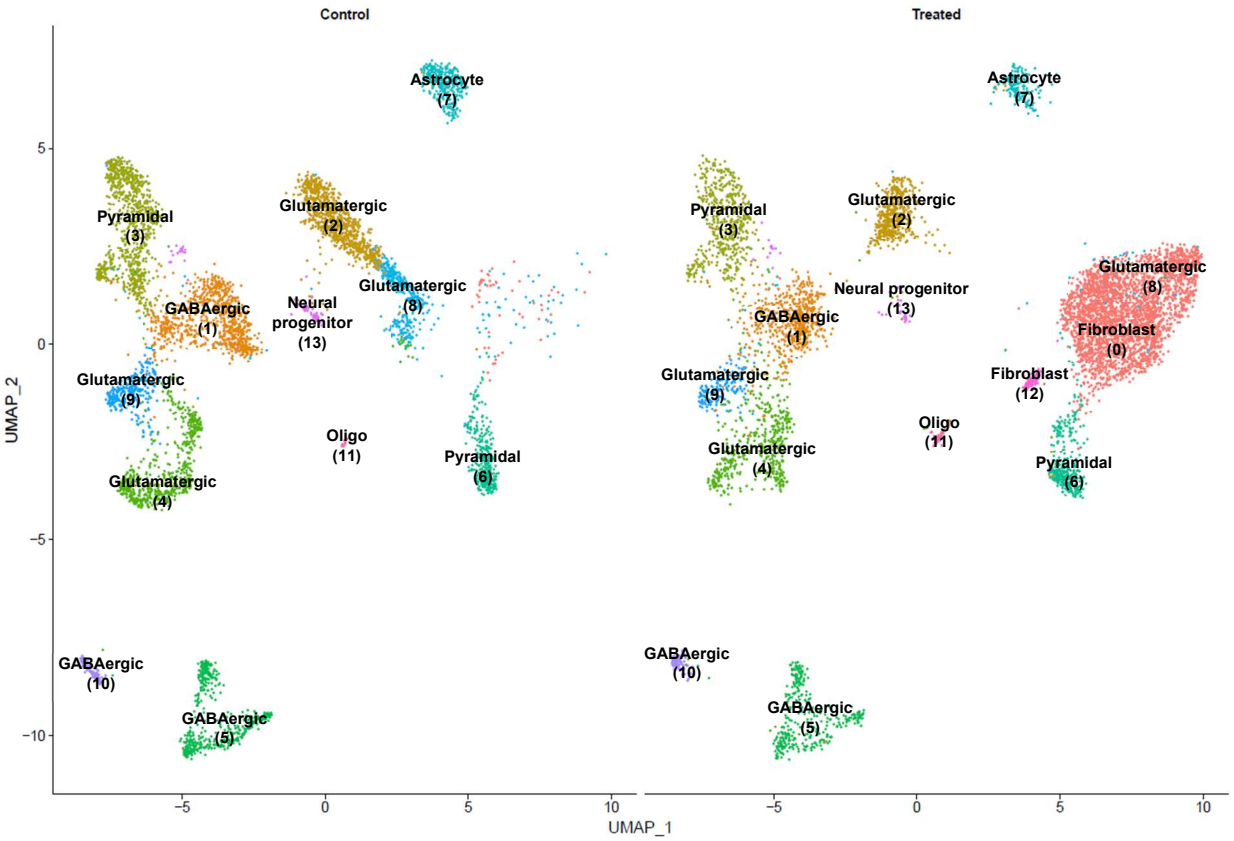

Figure 6. Annotated UMAP projection of Mouse 2 split by treatment. Fibroblast clusters (0 & 12) are only present in NC-RNP Ai14 guide "Treated" condition. Glutamatergic (8) cluster position is shifted between conditions, suggesting an NC-RNP effect that will be investigated in future analyses.

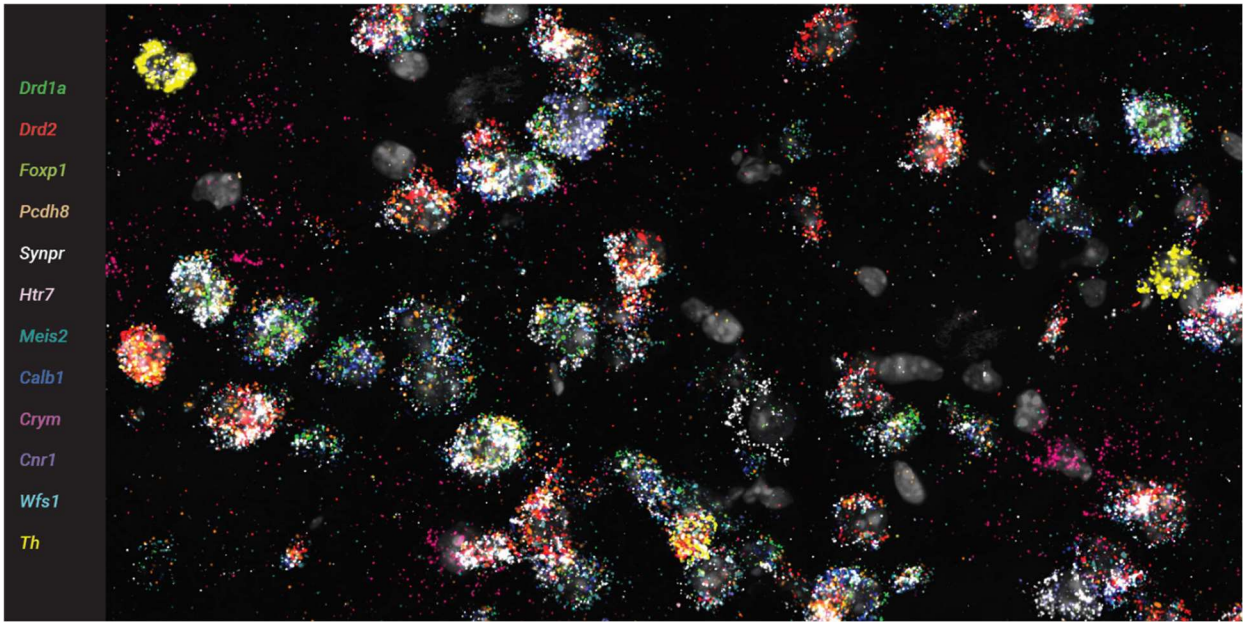

Figure 7. RNAscope HiPlex assay example workflow, visualizing D1 and D2 striatal medium spiny neurons in mouse brain (Phatak et al., 2019).

Methods:

Ai14 tdTomato Mouse Model

An Ai-14 mouse model was used to determine NC-RNP targeting efficiency *in vivo*. This model (Fig. 6) contains a tdTomato red fluorescent transgene that is downstream of a loxP-STOP cassette consisting of three *Sv40-polyA* sequences that prevents expression (Staahl et al., 2017). Excision of two or more poly(A) sequences by the NC-RNP induces a gain-of-function fluorescent signal that can be measured via microscopy and gene expression profiles.

Intracranial Injections and Isolation of Hippocampus Nuclei for Single Nuclei RNA-Sequencing

We have adapted a bilateral intracerebral injection protocol for rAAV into rat hippocampi for NC-RNP editing (Gerstein et al., 2013). The left hippocampi hemisphere was injected with our NC-RNP Ai14 targeting guide, while the right hemisphere received a NC-RNP scramble guide injection. Along with the NC-RNP Ai14 targeting guide, Mouse 1 was also injected with tdTomato expressing fibroblasts as a positive control. After repeating injections in a total of four mice, eight whole hippocampi were isolated in sucrose cutting solution according to a procotol described by Gimse et al. (2019), followed by homogenization in lysis buffer and isolation of nuclei following 10X Genomics' specifications.

Single Nuclei RNA-Sequencing Data Analysis

Sequenced gene expression libraires were aligned to an Ai14-tdTomato mouse custom reference genome using 10X Genomics' Cell Ranger. Cell count matrices were uploaded to R and analyzed following the standard Seurat 4.0.1. integration workflow (Stuart et al., 2019). Each loaded object was initially checked for "Ai14-tdTomato" gene using is.element, a function that searches the presence of elements within an object. The object features were normalized individually using NormalizeData function with "LogNormalize" method, which normalizes the gene expression levels for each cell by total expression, then multiplies them by 10,000, followed by log-transformation. Cells with unique feature counts less than 150 or greater than 2000 were excluded. Cells were not filtered for mitochondrial DNA levels, as DNA isolated from nuclei did not contain mtDNA. Variable gene features were identified individually using FindVariableFeatures function with default settings, and the FindIntegrationAnchors function

found pairs of cells across datasets that represent similar biological states to label as “anchors.” Datasets were integrated and scaled using ScaleData with default settings, which was followed by Principle Component Analysis dimensionality reduction using RunPCA function including 50 PCs. A UMAP projection was calculated using RunUMAP with all 50 PCs, and clusters were identified using FindNeighbors and FindClusters with default settings.

For cluster annotation, gene lists for each cluster were obtained and sorted first by adjusted p-value, excluding any genes $p>0.01$. The gene list was further sorted by log-fold change in expression (log_FC), where genes in each individual cluster were compared against all other clusters in the UMAP. The genes with the highest log_FC values were enriched using Azimuth and other cell marker databases. After cluster annotation, the positive control fibroblast clusters were removed by subsetting all other clusters as a separate Seurat object. The new object without the fibroblast cluster were then analyzed for tdTomato expression levels to reveal true expression by our NC-RNP.

References

Butler, A., Hoffman, P., Smibert, P., Papalexi, E., & Satija, R. (2018). Integrating single-cell transcriptomic data across different conditions, technologies, and species. *Nature Biotechnology*, *36*(5), 411–420. https://doi.org/10.1038/nbt.4096

Chen, G., Abdeen, A. A., Wang, Y., Shahi, P. K., Robertson, S., Xie, R., Suzuki, M., Pattnaik, B. R., Saha, K., & Gong, S. (2019). A biodegradable nanocapsule delivers a Cas9 ribonucleoprotein complex for in vivo genome editing. *Nature Nanotechnology*, *14*(10), 974–980. PubMed. https://doi.org/10.1038/s41565-019-0539-2

Gimse, K. E., O'Riordan, K., & Burger, C. (2019). Induction of Metabotropic Glutamate Receptor-Mediated Long-Term Depression in the Hippocampal Schaffer Collateral Pathway of Aging Rats. *Methods in Molecular Biology (Clifton, N.J.)*, *1941*, 93–105. https://doi.org/10.1007/978-1-4939-9077-1_8

Lein, E. S., Hawrylycz, M. J., Ao, N., Ayres, M., Bensinger, A., Bernard, A., … Jones, A. R. (2006). Genome-wide atlas of gene expression in the adult mouse brain. *Nature*, *445*(7124), 168–176. https://doi.org/10.1038/nature05453

Liang, X., Potter, J., Kumar, S., Zou, Y., Quintanilla, R., Sridharan, M., Carte, J., Chen, W., Roark, N., Ranganathan, S., Ravinder, N., & Chesnut, J. D. (2015). Rapid and highly efficient mammalian cell engineering via Cas9 protein transfection. *Journal of Biotechnology*, *208*, 44–53. https://doi.org/10.1016/j.jbiotec.2015.04.024

Miller, J. B., Zhang, S., Kos, P., Xiong, H., Zhou, K., Perelman, S. S., Zhu, H., & Siegwart, D. J. (2017). Non-Viral CRISPR/Cas Gene Editing In Vitro and In Vivo Enabled by Synthetic Nanoparticle Co-Delivery of Cas9 mRNA and sgRNA. *Angewandte Chemie (International Ed. in English)*, *56*(4), 1059–1063. PubMed. https://doi.org/10.1002/anie.201610209

Mout, R., Ray, M., Lee, Y.-W., Scaletti, F., & Rotello, V. M. (2017). In Vivo Delivery of CRISPR/Cas9 for Therapeutic Gene Editing: Progress and Challenges. *Bioconjugate Chemistry*, *28*(4), 880–884. PubMed. https://doi.org/10.1021/acs.bioconjchem.7b00057

Pérez-Martínez, F. C., Guerra, J., Posadas, I., & Ceña, V. (2011). Barriers to Non-Viral Vector-Mediated Gene Delivery in the Nervous System. *Pharmaceutical Research*, *28*(8), 1843–1858. https://doi.org/10.1007/s11095-010-0364-7

Phatak, J., Lu, H., Wang, L., Zong, H., May, C., Rouault, M., Qutaish, M., Zhang, B., Ma, Z., (2019). The RNAscope™ multiplex in situ hybridization technology enables the incorporation of spatial mapping and confirmation of gene signatures into single cell RNA sequencing workflows (Application Note). Retrieved from ACDBio: https://resources.bio-techne.com/bio-techne-assets/images/resources/mk-51-134-sscrna-seq-app-note.pdf

Sander, J. D., & Joung, J. K. (2014). CRISPR-Cas systems for editing, regulating and targeting genomes. *Nature Biotechnology*, *32*(4), 347–355. PubMed. https://doi.org/10.1038/nbt.2842

Sheldon, J., lu, han, Wang, L., & Ma, X. J. (2020). Incorporation of spatial mapping and confirmation of genes by single cell in situ hybridization technology into single cell RNA sequencing workflows. *Journal of Biomolecular Techniques : JBT*, *31*(Suppl), S13–S13. PMC.

Staahl, B. T., Benekareddy, M., Coulon-Bainier, C., Banfal, A. A., Floor, S. N., Sabo, J. K., Urnes, C., Munares, G. A., Ghosh, A., & Doudna, J. A. (2017). Efficient genome editing in the mouse brain by local delivery of engineered Cas9 ribonucleoprotein complexes. *Nature Biotechnology*, *35*(5), 431–434. PubMed. https://doi.org/10.1038/nbt.3806

Stuart, T., Butler, A., Hoffman, P., Hafemeister, C., Papalexi, E., Mauck, W. M., III, Hao, Y., Stoeckius, M., Smibert, P., & Satija, R. (2019). Comprehensive Integration of Single-Cell Data. *Cell*, *177*(7), 1888-1902.e21. https://doi.org/10.1016/j.cell.2019.05.031

Yao, Z., Liu, H., Xie, F., Fischer, S., Booeshaghi, A. S., Adkins, R. S., Aldridge, A. I., Ament, S. A., Pinto-Duarte, A., Bartlett, A., Behrens, M. M., Van den Berge, K., Bertagnolli, D., Biancalani, T., Corrada Bravo, H., Casper, T., Colantuoni, C., Creasy, H., Crichton, K., … Mukamel, E. A. (2020). An integrated transcriptomic and epigenomic atlas of mouse primary motor cortex cell types. *BioRxiv*, 2020.02.29.970558. https://doi.org/10.1101/2020.02.29.970558

Yin, H., Kauffman, K. J., & Anderson, D. G. (2017). Delivery technologies for genome editing. *Nature Reviews Drug Discovery*, *16*(6), 387–399. https://doi.org/10.1038/nrd.2016.280